

Metamaterial control of stimulated Brillouin scattering

M. J. A. Smith,^{1, 2,*} B. T. Kuhlmeij,¹ C. Martijn de Sterke,¹ C. Wolff,² M. Lapine,² and C. G. Poulton²

¹Centre for Ultrahigh bandwidth Devices for Optical Systems (CUDOS) and Institute of Photonics and Optical Science (IPOS), School of Physics, The University of Sydney, NSW 2006, Australia

²Centre for Ultrahigh bandwidth Devices for Optical Systems (CUDOS), School of Mathematical and Physical Sciences, University of Technology Sydney, NSW 2007, Australia

(Dated: June 11, 2019)

Using full opto-acoustic numerical simulations, we demonstrate enhancement and suppression of the SBS gain coefficient in a metamaterial comprising a subwavelength cubic array of dielectric spheres suspended in a dielectric background material. We develop a general theoretical framework and present several numerical examples for technologically important material combinations. For As_2S_3 spheres suspended in silicon, we achieve an enhancement of more than one order of magnitude in the SBS gain coefficient compared to pure silicon, and for GaAs spheres in silicon, perfect suppression of SBS is obtained. The gain coefficient for As_2S_3 glass can also be strongly suppressed by introducing a suspension of amorphous silica spheres. Effective photonic and acoustic parameters are shown to depend in a complex way on the filling fraction, and each have varying influence on the effective gain coefficient of the metamaterial. For the studied combinations of materials, electrostriction is the dominant effect behind the control of SBS in bulk media.

Stimulated Brillouin scattering (SBS) is a nonlinear scattering process whereby an incident electromagnetic pump field coherently drives an acoustic wave through the material, scattering the pump field and inducing a frequency shift in the returning, or Stokes, field [1–4]. This scattering process features prominently in nonlinear optics, due to its relevance in the design of nanoscale devices such as on-chip tuneable photonic filters, Brillouin lasers and sensors [2]. That said, SBS is also regarded as a nuisance in optical communications systems, with considerable effort being focused on techniques for its suppression [5]. The usual process by which sound is coherently excited in the medium for SBS is electrostriction [6, 7], which describes when an electric field induces a strain field in the material. These strains can coherently drive a longitudinal acoustic wave through the medium, inducing a periodic variation in the optical properties of the material (via the photoelastic effect). It is the combination of electrostriction and photoelasticity which scatters the incident optical field [2, 5, 6]; thus, materials with strong photoelastic and electrostrictive properties also tend to exhibit strong SBS. Conversely, materials with weak electrostriction and photoelasticity are poor candidates for experimental demonstrations of SBS.

A recent theoretical study by the authors [8] demonstrated that the electrostrictive response of a material can be considerably enhanced or suppressed through the introduction of a subwavelength cubic array of spheres in a background material. Such results suggest that SBS is also affected through subwavelength structuring. This is the motivation behind our study into how metamaterial structuring influences the SBS response.

In this work, we fully model the electrostrictive response of a metamaterial using perturbation procedures,

with very few restrictive assumptions. The metamaterial we consider is a cubic array of spheres embedded in a background material. In contrast to existing work [8] which gave an analytical expression for the electrostriction within a hydrostatic approximation, we incorporate shear effects in our model (which are generally non-negligible in solid media but can easily be omitted for liquids). To evaluate the SBS gain, we also evaluate other photonic and acoustic parameters in the subwavelength limit, and incorporate the effects of acoustic loss. To the best of our knowledge, this is the first investigation on the SBS behaviour of metamaterials and we emphasise that the results presented are for intrinsic, or bulk, SBS properties. We theoretically obtain effective values for all material parameters which feature in the SBS gain coefficient, all of which vary differently as we tune the filling fraction of our metamaterial and investigate different material combinations.

In addition to outlining a general theoretical framework, we present numerical results for a selection of silicon and chalcogenide glass-based metamaterials, to demonstrate suppression and enhancement of the intrinsic SBS gain coefficient. There is considerable interest in silicon-based materials due to a wide range of potential applications in the electronics industry, as silicon is CMOS-compatible [2]. That said, the biggest drawbacks in the use of conventional silicon as an SBS material are its inherently poor SBS gain coefficient, high speed of sound, and its large acoustic losses. We overcome these issues by introducing a suspension of spheres in the background material, and demonstrate an order of magnitude enhancement in the gain coefficient of bulk silicon using chalcogenide glass spheres. We also show absolute suppression of SBS in silicon using GaAs spheres.

The example we present for an As_2S_3 background material shows strong suppression in the SBS gain coefficient when structured with a cubic lattice of silica spheres, which means that SBS would be observed at much higher

* m.smith@physics.usyd.edu.au

TABLE I. Bulk material parameters including refractive index n , photoelastic tensor coefficients p_{ij} , Brillouin frequency shift $\Omega_B/(2\pi)$ (units of [GHz]), linewidth $\Gamma_B/(2\pi)$ (units of [MHz]), gain coefficient g_P (units of [$\text{m} \cdot \text{W}^{-1}$]), phonon viscosity coefficients η_{ij} (units of [$\text{mPa} \cdot \text{s}$]), stiffness tensor coefficients C_{ij} (units of [GPa]), material density ρ (units of [$\text{kg} \cdot \text{m}^{-3}$]), and acoustic velocity V_A (units of [$\text{m} \cdot \text{s}^{-1}$]) [9–15], where \dagger denotes theoretical estimates and subscripts are in Voigt form.

Material	n	p_{11}	p_{12}	p_{44}	$\frac{\Omega_B}{2\pi}$	$\frac{\Gamma_B}{2\pi}$	max (g_P)	η_{11}	η_{12}	η_{44}	C_{11}	C_{12}	C_{44}	ρ	V_A
Fused SiO ₂	1.45	0.12	0.27	-0.075	11.1	16	4.52×10^{-11}	1.6 [†]	1.29 [†]	0.16 [†]	78.6	16.1	31.2	2200	5960
As ₂ S ₃	2.37	0.25	0.24	0.005	7.95	34	0.74×10^{-9}	1.8 [†]	1.45 [†]	0.18 [†]	18.7	6.1	6.4	3200	2595
Si [100]	3.48	-0.09	0.017	-0.051	38 [†]	320 [†]	2.4×10^{-12} [†]	5.9	5.16	0.62	165.6	63.9	79.5	2329	8433
GaAs [100]	3.37	-0.165	-0.14	-0.072	21 [†]	167 [†]	0.2×10^{-9} [†]	7.49	6.57	0.72	119	53.4	59.6	5320	4734

laser powers (i.e. this increases the SBS threshold). Demonstrating SBS suppression in isotropic materials is relevant to those studying other nonlinear optical effects in common laser glasses, such as four-wave mixing, where undesired SBS effects can dominate.

The procedure for deriving the coupled intensity equations for electrostriction-induced SBS is well-known [3, 4, 16], and considers optical plane wave propagation in an isotropic bulk material. It ultimately gives rise to the coupled system

$$\partial_z I_1 = -g_P I_1 I_2, \quad \partial_z I_2 = g_P I_1 I_2, \quad (1)$$

where the SBS power gain factor is given by

$$g_P = \frac{4\pi^2\gamma^2}{nc\lambda_1^2\rho V_A \Gamma_B} \left(\frac{(\Gamma_B/2)^2}{(\Omega_B - \Omega)^2 + (\Gamma_B/2)^2} \right). \quad (2)$$

Here $I_{1,2}$ denote the intensities of the incident pump and Stokes field, respectively, ε_0 is the vacuum permittivity, n is the refractive index, c is the speed of light in vacuum, γ is a measure of the electrostrictive stress in the medium (see below), λ_1 is the incident optical wavelength in vacuum, ρ is the mean material density, V_A is the longitudinal acoustic wave velocity, Ω is the angular frequency of the acoustic wave, Ω_B denotes the Brillouin frequency shift, and Γ_B is the Brillouin line width at half maximum, with respect to angular frequency. Note that a conventional backwards SBS process has $\Omega_B = q_B V_A \approx 2\omega_1 n V_A / c$ where $\mathbf{q}_B = 2\mathbf{k}_1$ is the corresponding wave vector [3, 4] and ω_1 is the angular frequency of the incident optical field. The expression for γ is typically given in terms of the photoelastic tensor p_{ijkl} which is defined in Einstein notation by [17]

$$\Delta(\varepsilon_{ij}^{-1}) = p_{ijkl} s_{kl}, \quad (3)$$

where ε_{ij} is the relative permittivity tensor, $s_{ij} = \frac{1}{2}(\partial_i u_j + \partial_j u_i)$ is the strain tensor, u_i is the elastic displacement from equilibrium, and Δ denotes the change resulting from the strain. In this setting we have [5, 18]

$$\gamma = \gamma_{xx} = \varepsilon_r^2 p_{xxxy}. \quad (4)$$

Consequently, provided that effective medium descriptions are obtained for each parameter in (2) above, we can determine the gain coefficient and characterise the

SBS properties of a metamaterial. For reference, a range of material parameters [9–15] are shown in Table I.

We now proceed to obtain effective parameters for all material parameters in (2)–(4), beginning with an effective permittivity. For reference, we specify the unit cell to be symmetric about the origin, defining d as the period of the cubic lattice, and a as the radius of the sphere, from which we define the filling fraction as $f = 4\pi a^3/(3d^3)$. The effective permittivity tensor is obtained here for a metamaterial using a modification of the procedure outlined in [19], which is chosen for its conceptual simplicity and ease of numerical implementation (in this work, all problems are solved using a commercial finite element solver). This method involves first solving the eigenvalue problem for Maxwell's equations for a number of sub-wavelength Bloch vectors. For each vector we compute the volume averaged energy density [20]

$$U_{\text{avg}} = \frac{1}{2} \frac{1}{V_{\text{WSC}}} \varepsilon_0 \langle \varepsilon_{ij} |E_j|^2 \rangle, \quad (5)$$

where E_j is the electric field distribution of the Bloch mode, V_{WSC} is the volume of the Wigner-Seitz cell, and $\langle \rangle$ denotes volume integration. This quantity is then equated to the effective energy density expression

$$U_{\text{eff}} = \frac{1}{2} \frac{1}{(V_{\text{WSC}})^2} \varepsilon_0 \varepsilon_{ij}^{\text{eff}} |\langle E_j \rangle|^2, \quad (6)$$

giving rise to a linear system that is solved directly for the effective permittivity tensor. For example, an optically anisotropic material where the principal axis of the effective system is aligned with the Cartesian coordinate system has

$$\varepsilon_{xx}^{\text{eff}} |\langle E_x \rangle|^2 + \varepsilon_{yy}^{\text{eff}} |\langle E_y \rangle|^2 + \varepsilon_{zz}^{\text{eff}} |\langle E_z \rangle|^2 = V_{\text{WSC}} \langle \varepsilon_{ij} E_i E_j^* \rangle, \quad (7)$$

and a 3×3 linear system is obtained by choosing different Bloch vectors in the vicinity of the Γ point and evaluating (7) each time. Following (4) we now determine the effective photoelastic constant p_{xxxy}^{eff} . This is obtained by mechanically perturbing the unit cell to approximate a strain induced by a longitudinal acoustic wave propagating through the metamaterial. Thus, we solve the acoustic wave equation [6] with zero body forces

$$-\rho \partial_t^2 u_i + \partial_j (C_{ijkl} \partial_k) u_l = 0, \quad \text{for } i = x, y, z, \quad (8)$$

inside the unit cell, assuming we are in the vicinity of Γ (i.e. we impose a time dependence of $\exp(-i\Omega t)$ where Ω is in the long wavelength limit). Here C_{ijkl} denotes the stiffness tensor. To model the compression of the unit cell by the acoustic wave, we impose the boundary conditions

$$u_j|_{\partial W_{\pm z}} = -Dz\delta_{zj}|_{\partial W_{\pm z}}, \quad u_j n_j|_{\partial W \setminus \{\partial W_{\pm z}\}} = 0, \quad (9)$$

where ∂W denotes the boundary of the entire unit cell, D is the magnitude of the displacement, n_j are the components of the local normal vector to the surface, $\partial W_{\pm z}$ denote the faces of the cube with normal vectors $n_j = \pm\delta_{zj}$, and δ_{ij} is the Kronecker delta. This boundary condition generates a compressed unit cell geometry and an internal strain field which modifies the constituent permittivity tensors, making them spatially dependent (see (3)). Next, we repeat the procedure outlined in (5)–(6) to obtain an effective permittivity for the strained configuration, using the strained constituent permittivities. Having determined the strained and unstrained effective permittivity tensors (corresponding to an imposed strain over the unit cell of $s_{zz} = -2D/d$), the p_{xxyy}^{eff} coefficient for the metamaterial follows directly from the analogue to (3), after using the symmetry properties of cubic crystals [21].

To determine the remaining effective parameters: the acoustic velocity and Brillouin linewidth, we examine the acoustic properties of the unstrained metamaterial. That is, we consider the acoustic wave equation (8) under the assumption of time-harmonic fields taken in the long wavelength limit. In this setting, the effective acoustic wave velocity is obtained directly by solving the acoustic eigenvalue problem and evaluating $V_A^{\text{eff}} = \tilde{\Omega}/\tilde{q}$, where $\tilde{\mathbf{q}} = 2\mathbf{k}_1 = (0, 0, 4\pi n_{\text{eff}}/\lambda_1)$ is the SBS resonant wave vector with corresponding acoustic frequency $\tilde{\Omega}$ and longitudinal mode \tilde{u}_j . We calculate the effects of acoustic loss using perturbation theory; we substitute $C_{ijkl} + \eta_{ijkl}\partial_t$ for C_{ijkl} in (8), where η_{ijkl} is the phonon dynamic viscosity tensor [6, 15]. Subsequently acoustic frequencies are perturbed as

$$\tilde{\Omega}^2 \rightarrow \tilde{\Omega}^2 + i\tilde{\Omega} \frac{\langle a_j \tilde{u}_j^* \rangle}{\langle \rho \tilde{u}_j \tilde{u}_j^* \rangle}, \quad (10)$$

where $a_i = \partial_j(\eta_{ijkl}\partial_k \tilde{u}_l)$. Numerically evaluating the square root of (10) one obtains $\tilde{\Omega} \rightarrow \tilde{\Omega}_R - i\tilde{\Omega}_I$ from which $\Omega_B^{\text{eff}} = \tilde{\Omega}_R$ and $\Gamma_B^{\text{eff}} = 2\tilde{\Omega}_I$ immediately follows [20]. We note that in order to evaluate the effective linewidth of a metamaterial one must possess the η_{ijkl} of the constituent materials, and these are generally not well-tabulated. For uniform materials where η_{ijkl} are not available, estimates are obtained by using results from SBS experiments [10, 13] and imposing $u_j = \exp(iqz - i\Omega t)\delta_{zj}$ to obtain $\tilde{\Omega}^2 \rightarrow \tilde{\Omega}^2 - i\tilde{\Omega}q^2\eta_{zzzz}/\rho$. Taking the square root of both sides and evaluating a Taylor series in q ultimately gives

$$\eta_{zzzz} \approx \frac{V_A^2 \Gamma_B \rho}{\Omega_B^2}. \quad (11)$$

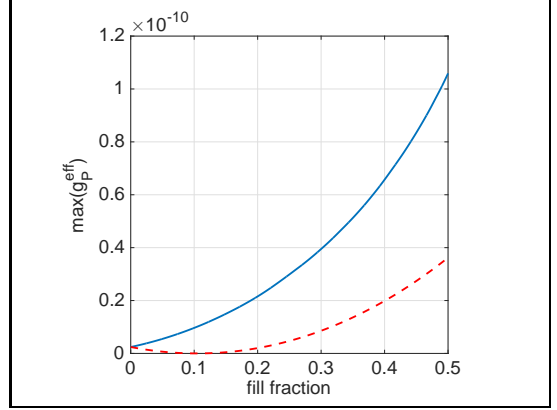


FIG. 1. Effective gain coefficient for cubic lattice of As_2S_3 spheres in Si (blue) and GaAs spheres in Si (broken red) at $\lambda_1 = 1550$ nm for $d = 50$ nm.

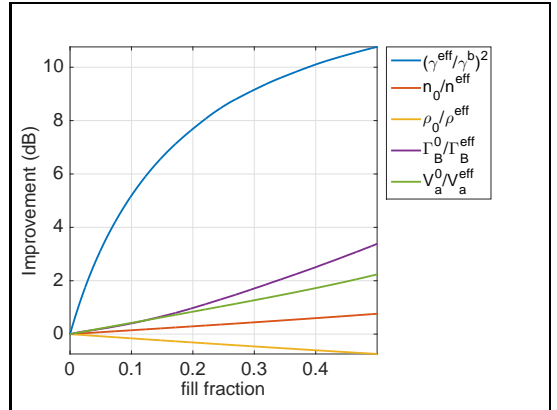


FIG. 2. Contribution from each effective material parameter to improvement in g_P^{eff} for As_2S_3 spheres in Si.

Following experimental data on η_{ijkl} [15] we estimate η_{yzyz} as being one order of magnitude smaller than η_{zzzz} , and assuming the material is isotropic, the identity $\eta_{yzyz} = \frac{1}{2}(\eta_{xxxx} - \eta_{xxyy})$ gives η_{xxyy} . Note that estimated values presented in Table I are denoted by \dagger .

Having described the numerical procedures for determining all of the effective parameters of the metamaterial, we now consider a selection of illustrative examples. For each choice of pairwise material combination, we consider the maximum gain coefficient (2) against the filling fraction (where the maximum filling fraction for a cubic lattice of spheres is $f = \pi/6 \approx 0.52$). We also consider how each parameter in (2) contributes to the effective gain coefficient by evaluating

$$10 \log_{10} \left(\frac{\max(g_P^{\text{eff}})}{\max(g_P^b)} \right) = 10 \log_{10} \left(\left(\frac{\gamma}{\gamma^b} \right)^2 \right) + \dots$$

and superposing a plot of all logarithmic terms in a single figure (where b denotes the background material). In this way, the contribution from each parameter is apparent because the improvement in the gain coefficient (in

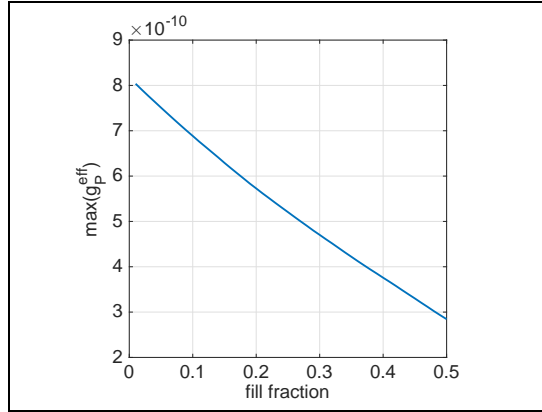


FIG. 3. Effective gain coefficient for a cubic lattice of SiO_2 spheres in As_2S_3 at $\lambda_1 = 1550$ nm for $d = 50$ nm.

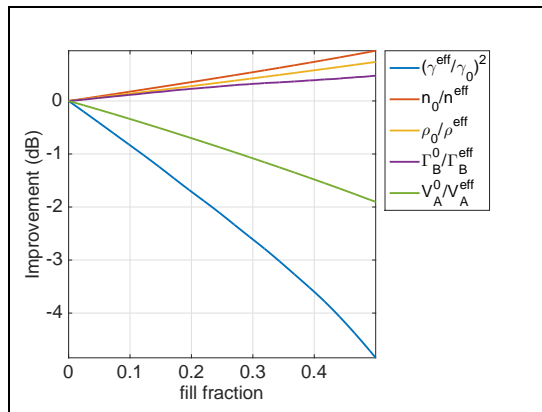


FIG. 4. Contribution from each effective material parameter to improvement in g_P^{eff} for SiO_2 spheres in As_2S_3 (Figure 3).

dB) is then the sum of each curve value at a given filling fraction. In Figure 1, we present the effective gain coefficient for a cubic lattice of As_2S_3 spheres in Si at $\lambda_1 = 1550$ nm, where the lattice period is $d = 50$ nm (solid blue curve). The period of the lattice is chosen to ensure that all effective material parameters are optically and acoustically subwavelength for all fill fractions: for the examples considered here, we have approximately 10 unit cells per optical wavelength. From Figure 1 we see that As_2S_3 spheres in Si gives an order of magnitude enhancement in the SBS gain ((2)) from the bulk Si value shown in Table I. In this case, an enhancement factor of more than 40 is achieved at $f = 50\%$ where $\max(g_P^{\text{eff}}) = 1.06 \times 10^{-10} \text{ m} \cdot \text{W}^{-1}$, which is more than twice that of pure fused SiO_2 (here we also have $\Gamma_B^{\text{eff}}/(2\pi) = 147$ MHz and $\Omega_B^{\text{eff}}/(2\pi) = 18$ GHz). In Figure 2, we observe that the SBS gain enhancement is largely driven by an increase in electrostriction, which is greater than the contributions from improvements in the refractive index, acoustic velocity, and Brillouin linewidth combined. Note that the increasing

density of the metamaterial drives a decrease in the gain coefficient, but for this example, only slightly mitigates the improvements from the other parameters.

Also shown in Figure 1 is the effective gain coefficient for GaAs spheres in Si where complete suppression of SBS is achieved at a filling fraction of $f = 10\%$, and a $\max(g_P^{\text{eff}}) = 3.6 \times 10^{-11} \text{ m} \cdot \text{W}^{-1}$ is achieved at $f = 50\%$. Note that at $f = 50\%$ we have structured Si with GaAs to obtain a gain coefficient comparable to pure fused SiO_2 , albeit with a broader linewidth of $\Gamma_B^{\text{eff}}/(2\pi) = 223$ MHz and a greater frequency shift of $\Omega_B^{\text{eff}}/(2\pi) = 27$ GHz. Analogously to the example with As_2S_3 spheres in Si, the SBS gain for GaAs spheres in Si for $f > 10\%$ is driven by enhancements in all parameters except for the effective material density (not shown). The $g_P^{\text{eff}} = 0$ observed at $f = 10\%$ is caused by $p_{\text{xxyy}}^{\text{eff}} = 0$, which is in turn due to a sign change in constituent p_{xxyy} values (see Table I).

In Figure 3 we show the effective gain coefficient for SiO_2 spheres in As_2S_3 , which demonstrates a more than 60% suppression in the gain coefficient at $f = 50\%$ (with corresponding values $\max(g_P^{\text{eff}}) = 0.28 \times 10^{-9} \text{ m} \cdot \text{W}^{-1}$, $\Gamma_B^{\text{eff}}/(2\pi) = 30$ MHz and $\Omega_B^{\text{eff}}/(2\pi) = 9$ GHz). The explanation for this suppression is found in Figure 4 where reductions in the effective electrostriction and acoustic velocity outstrip positive contributions from all other remaining parameters. This points to the acoustic velocity playing an important role in the suppression of SBS in metamaterials, in addition to the electrostriction. Note our calculated value for the intrinsic SBS gain coefficient of As_2S_3 (i.e., at $f = 0\%$) is within 10% of the experimental value in Table I.

In summary, we have shown that both considerable enhancement and full suppression of SBS in silicon is achieved through a careful choice of inclusion material in a metamaterial comprising spheres in a cubic lattice. The procedures outlined here for determining the effective photonic and acoustic parameters at long wavelengths can be extended to consider other more complicated metamaterial designs, and will be used in future studies of this type. The methods are also rigorous, as effective material parameters are evaluated with minimal assumptions. The enhancement of the silicon gain coefficient to values greater than, or comparative to, fused silica is particularly promising for designers of small-scale, silicon based SBS devices. There is also considerable scope for metamaterials where the acoustic velocity contrast and the Brillouin linewidth contrast is high, as the contributions of these parameters have been shown here to play an important role in controlling SBS.

ACKNOWLEDGEMENTS

This work was supported by the Australian Research Council (CUDOS Centre of Excellence, CE110001018).

[1] R. W. Boyd, K. Rzążewski, and P. Narum, Phys. Rev. A **42**, 5514 (1990).

[2] B. J. Eggleton, C. G. Poulton, and R. Pant, Adv. Opt. Photonics **5**, 536 (2013).

[3] P. E. Powers, *Fundamentals of nonlinear optics* (CRC Press, Boca Raton, 2011).

[4] A. Kobyakov, M. Sauer, and D. Chowdhury, Adv. Opt. Photonics **2**, 1 (2010).

[5] E. Peral and A. Yariv, IEEE J. Quantum Elect. **35**, 1185 (1999).

[6] B. A. Auld, *Acoustic fields and waves in solids* (John Wiley & Sons, 1973).

[7] C. Wolff, M. J. Steel, B. J. Eggleton, and C. G. Poulton, Phys. Rev. A **92**, 013836 (2015).

[8] M. J. A. Smith, B. T. Kuhlmeij, C. M. de Sterke, C. Wolff, M. Lapine, and C. G. Poulton, Phys. Rev. B **91**, 214102 (2015).

[9] M. J. Weber, *Handbook of optical materials* (CRC press, Boca Raton, 2002).

[10] K. S. Abedin, Opt. Expr. **13**, 10266 (2005).

[11] J. M. Rouvaen, E. Bridoux, M. Moriamez, and R. Torguet, App. Phys. Lett. **25**, 97 (1974).

[12] R. K. Galkiewicz and J. Tauc, Solid State Commun. **10**, 1261 (1972).

[13] R. Pant, C. G. Poulton, D. Y. Choi, H. Mcfarlane, S. Hile, E. Li, L. Thevenaz, B. Luther-Davies, S. J. Madden, and B. J. Eggleton, Opt. Expr. **19**, 8285 (2011).

[14] D. K. Biegelsen, Phys. Rev. Lett. **32**, 1196 (1974).

[15] B. G. Helme and P. J. King, Phys. Status Solidi A. **45**, K33 (1978).

[16] G. P. Agrawal, *Nonlinear fiber optics*, 2nd ed. (Academic press, San Diego, 1995).

[17] R. E. Newnham, *Properties of Materials: Anisotropy, Symmetry, Structure: Anisotropy, Symmetry, Structure* (Oxford University Press, New York, 2004).

[18] P. T. Rakich, P. Davids, and Z. Wang, Opt. Expr. **18**, 14439 (2010).

[19] D. J. Bergman, Phys. Rep. **43**, 377 (1978).

[20] J. D. Jackson, *Classical Electrodynamics*, 2nd ed. (Wiley, New York, 1962).

[21] J. F. Nye, *Physical properties of crystals: their representation by tensors and matrices* (Oxford university press, Suffolk, 1985).